A scanning tunnelling microscopy study of C and N adsorption phases on the vicinal Ni(100) surfaces Ni(810) and Ni(911)

S.M. Driver[+], R.L. Toomes and D.P. Woodruff[*]

Physics Department, University of Warwick, Coventry CV4 7AL, UK

Abstract

The influence of N and C chemisorption on the morphology and local structure of nominal Ni(810) and Ni(911) surfaces, both vicinal to (100) but with [001] and [01$\bar{1}$] step directions respectively, has been investigated using scanning tunnelling microscopy (STM) and low energy electron diffraction. Ni(911) undergoes substantial step bunching in the presence of both adsorbates, with the (911)/N surface showing (411) facets, whereas for Ni(810), multiple steps 2-4 layers high are more typical. STM atomic-scale images show the (2x2)pg 'clock' reconstruction on the (100) terraces of the (810) surfaces with both C and N, although a second c(2x2) structure, most readily reconciled with a 'rumpling' reconstruction, is also seen on Ni(810)/N. On Ni(911) the clock reconstruction is not seen on the (100) terraces with either adsorbate, and these images are typified by protrusions on a (1x1) mesh. This absence of clock reconstruction is attributed to the different constraints imposed on the lateral movements of the surface Ni atoms adjacent to the up-step edge of the terraces with a [01$\bar{1}$] step direction.

Keywords: surface structure; surface reconstruction; vicinal surfaces; stepped surfaces; nickel; carbon; nitrogen; adsorption

---

[+] now at Chemistry Department, University of Cambridge, Cambridge CB2 1EW, UK

[*] corresponding author, email: d.p.woodruff@warwick.ac.uk fax: +44 24 76692016

1. Introduction

It is now widely recognised that in adsorption onto solid surfaces the outermost substrate layer does not behave as a simple rigid atomic chequer board, but is modified structurally by the adsorption. In some cases this effect may be quite subtle, such as small changes in the outermost substrate layer spacing, or slight 'rumpling' (relative displacements perpendicular to the surface within a single atomic layer) of one or more of these layers to distinguish atoms below, or not below, the adsorbate. In other cases more substantial movements of the atoms in the outermost layers occur, sometimes decreasing or increasing the atomic density of one or more layers. Probably the earliest demonstrated example of this phenomenon of adsorbate-induced surface reconstruction is the so-called 'clock'-reconstructed Ni(100)(2x2)-C pg surface phase [1]. In this structure C atoms adsorb to occupy alternate four-fold coordinated hollow sites on the (100) surface with c(2x2) periodicity, but the four nearest neighbour Ni atoms to each carbon atom expand outwards from the adsorbate and rotate azimuthally in alternate clockwise and anticlockwise directions to produce an interlocking structure with (2x2) periodicity (see Fig. 1 – note that the magnitude of the displacements is exaggerated in this figure for clarity). This structure has characteristic glide symmetry planes which give rise to extinctions of all diffracted beams of the type (n + ½, 0) and (0, n + ½) when viewed at normal incidence by a diffraction technique such as low energy electron diffraction (LEED).

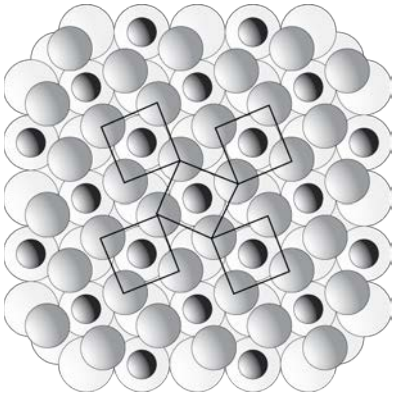

Fig. 1 Schematic diagram of the Ni(100)(2x2) pg 'clock' structure induced by C or N. For clarity the surface layer Ni atoms are shown as smaller darker shaded spheres than the underlayer Ni atoms and the lateral distortion is exaggerated in magnitude. The overlaid lines highlight the characteristic clockwise and counter-clockwise rotated square groups of four Ni atoms that are also seen in STM images.

The existence of this structure was first proposed on the basis of an early multiple-scattering LEED intensity-energy study [1], but the quantitative details of the structure have subsequently been determined by more modern versions of this [2] and other methods [3, 4]. Direct evidence of this qualitative behaviour has also been provided by scanning tunnelling microscopy (STM) [5]. Subsequently it was shown that a similar 'clock reconstruction' is formed by 0.5 ML of atomic N on Ni(100) [6], deposited either from NH_3 dissociation or by using low energy ion bombardment from N_2 gas, followed by low temperature annealing to remove the damage and the excess buried nitrogen. By contrast, atomic oxygen also forms a 0.5 ML overlayer on Ni(100), but in this case the structure has the simpler c(2x2) periodicity with no lateral distortion of the Ni surface layer.

There have been quite a number of investigations aimed at trying to understand why this (2x2) pg reconstruction is induced by a c(2x2) overlayer of C and N, but not O (see, for example, the discussion and references cited in [4, 7], and somewhat more recent papers [8, 9]). In the reconstructed phases both C and N occupy sites almost coplanar with the outermost Ni layer, while adsorbed oxygen is some 0.8 Å above this layer, so one rationale is that the slightly smaller C and N atoms are able to penetrate the surface layer to bond to the underlying second layer Ni atom, but only by slightly enlarging the hollow site in the surface Ni layer. Experimental measurements of the increase in compressive surface stress induced by the adsorption of C and O have shown that the rate of increase with coverage is greater for C, and this increase ceases as the reconstruction occurs [10]. In the case of the C adsorbate, STM data at low coverage was interpreted as indicating that a precursor to the reconstruction was an outward relaxation of the nearest neighbour Ni atoms [5], but a quantitative local structure determination indicated any such strain is negligible [4]. Nevertheless, it is generally recognised that surface stress plays a role in driving the reconstruction (whatever the origins of this stress). Of course, one rather striking feature of this reconstruction (fig. 1) is that it requires concerted lateral displacements of many atoms over an extended surface, which is strongly constrained by the close packing of the surface layer. This raises an interesting question: if these

constraints on lateral strain are relaxed, at least locally, by the presence of an atomic step, would the behaviour be different?

The present investigation is motivated by the desire to try to answer this question. We have conducted an investigation of the changes in surface structure and morphology induced by C and N on Ni(100) vicinal surfaces with average step directions along the two principal azimuths, [01$\bar{1}$] and [001], corresponding to close-packed and more open step structures, using STM. Of course, STM does not provide quantitative structural information, and the interpretation of atomic-scale images on adsorbate-covered metal surfaces is not without its difficulties, but we can search for systematic differences in the atomic imaging of the (100) terraces on these vicinal surfaces. We should note that a study of the effects of N adsorption on a range of vicinal Ni(100) surfaces in the [001] zone using qualitative LEED, evidently motivated by the same question, has already been reported [11]. STM can provide rather more direct and local structural information, but we have also performed some LEED characterisation of our surfaces which provides a useful comparison to the earlier work. STM also allows one to study morphological changes such as step-bunching and faceting (on a nanometre scale) which can often occur as a result of adsorption. Indeed, such morphological changes may be of significant practical interest in the case of C adsorption, as surface C is known to be present on Ni surfaces during the methanation reaction [12], so the shape of small catalyst particles under reaction conditions could be markedly influenced by such processes.

2. Experimental Details

The nominally Ni(810) and Ni(911) samples were prepared by spark machining from a single crystal bar oriented using Laue X-ray diffraction, followed by mechanical polishing using successively finer grades of diamond paste. Fig. 2 shows schematic diagrams of the ideal termination of these faces. Notice, of course, that small variations in the exact angle of the face can impact significantly on the exact atomic structure; changes in the tilt angle within the correct rotational plane will lead to variations of the step spacing, but small twists of this rotational plane will introduce kinks into the steps. The

cutting procedure typically achieves approximately 1° accuracy in the tilt angle, but the azimuthal orientation is almost certainly less precise.

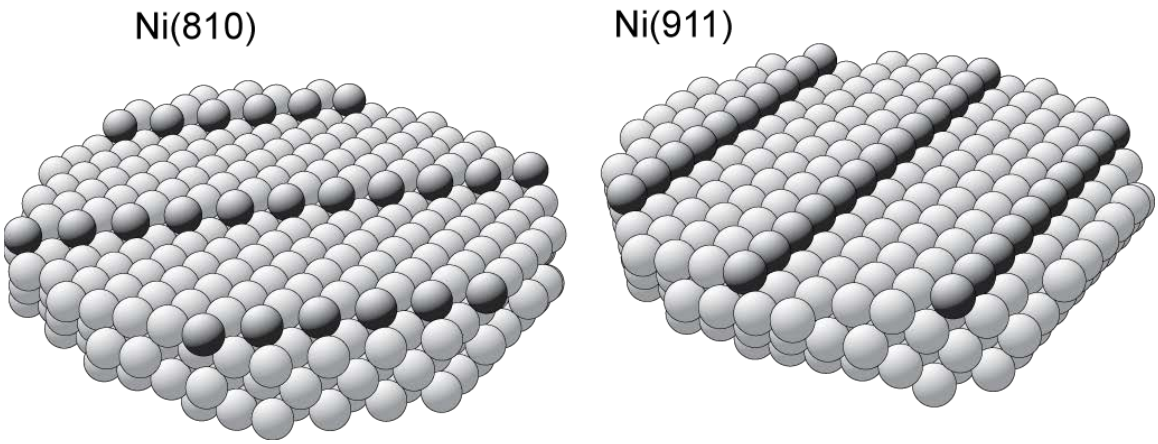

Fig. 2 Schematic diagram of the ideal Ni(810) and Ni(911) surfaces. The atoms along the steps (the down-step edges of the terraces) are shaded darker for clarity.

After inserting into the ultra-high vacuum (UHV) chamber, the samples were cleaned by repeated cycles of Ar^+ ion bombardment and annealing until a sharp (1x1) LEED pattern was obtained and no sign of contamination was seen in the Auger electron spectrum. Nitrogen overlayers were prepared by nitrogen ion bombardment at 500 eV over a range of doses (typically a few hundred μC) according to the coverage required, followed by annealing to 300-375°C. C deposition was effected by exposing the surfaces to approximately $120x10^{-6}$ mbar.s of acetylene at a sample temperature of 250°C. The objective in these dosing procedures was to achieve a nominal saturation of the chemisorbed phases which, on extended Ni(100) terraces, occurs at 0.5 ML. LEED showed the appearance of additional (2x2) diffraction beams. Auger electron spectroscopy confirmed the presence of surface C or N with no evidence of the presence of contaminant species.

The STM experiments were conducted at room temperature using an Omicron Vakuumphysik 'micro-STM' mounted on a spring and magnetic eddy current damping system in UHV. Electrochemically etched polycrystalline W tips were used, conditioned in situ by Ar^+ ion bombardment. These were then subjected to field desorption (-300 V

sample bias) against a clean Cu surface and to gap voltage pulses (x10) during scanning, in order to clean the tip or to modify its condition to alter the resolution obtained, as discussed below. Images were recorded using the standard constant tunnelling current mode. Tunnelling parameters are given in the figure captions, low gap resistances being typical. The azimuthal orientation of each image depends on the chosen scan angle (the angle of the fast scan direction anticlockwise from the nominal x-direction of the piezo-tube scanner) and is also affected by some rotational freedom of the sample stage in the STM. Small amounts of thermal drift and piezo creep, for which we have not corrected, may cause slight distortions of angles and lengths in the images.

Notice that the presentation of atomic-scale images from the individual (100) terraces of these vicinal surfaces requires some special treatment. Particularly in the presence of bunched steps of multiple atomic layer spacings, and small facets, images that are levelled to the average surface orientation (the standard procedure in STM) include height variations of many atomic spacings. This means that the small height variations associated with atomic corrugations on the terraces are difficult to discern. A further problem is that it difficult, in the case of step bunching, to identify correctly the exact location of individual steps. There are several alternative solutions to this problem. One way to gain clearer information on the atomic corrugations within an individual (100) terrace is to level the image to the (100) terrace orientation and expand the grey scale to cover the variations in height on a single terrace (other terraces becoming entirely white or entirely black). An alternative is to apply a high-pass filter to the scanned images which removes the gradual height changes across terraces.

A third possibility, which we have adopted in the majority of the images presented here, retains the clarity and underlying simplicity of the single-terrace levelling approach, but allows atomic-scale information on multiple terraces to be visualised, and also provides clear information on the location of the atomic steps. In this method we apply co-levelling of successive terraces in an image, using software processing. Perpendicular offsets relative to these terraces (set to be integral multiples of one layer spacing) are added or subtracted to each terrace in turn, to bring all terraces to the same horizontal

plane. The greyscale can then be expanded to optimise contrast in the atomic-scale detail within the terraces. A sharp white/black boundary is seen on passing over a step from a lower to a higher terrace. Clearly this means that the image is ‘distorted’ at the step edge, but a systematic choice of vertical cut-off points (half-way between the average levels of the lower and higher terraces) provides a consistent marker of nominal step positions, and the number of levels in a multiple-height step can be counted easily. This method also offers a particularly reliable means of dealing with any uncertainty in the calibration of the scanner's scaling perpendicular to the surface. Fig. 3 provides an example of an image from the Ni(810)/N surface treated in this way and compared with the same image levelled to the average surface plane and subjected to high-pass filtering. Important advantages of this mode of display, evident in this example, include a particularly clear identification of atomic steps and undistorted imaging of features within the co-levelled terraces; the only distortion in detail is localised at the step edges. Notice that these images also allow easy identification of the up-step and down-step directions in the images; the upper side of a step is marked by a dark strip and the lower side of the step by a bright strip.

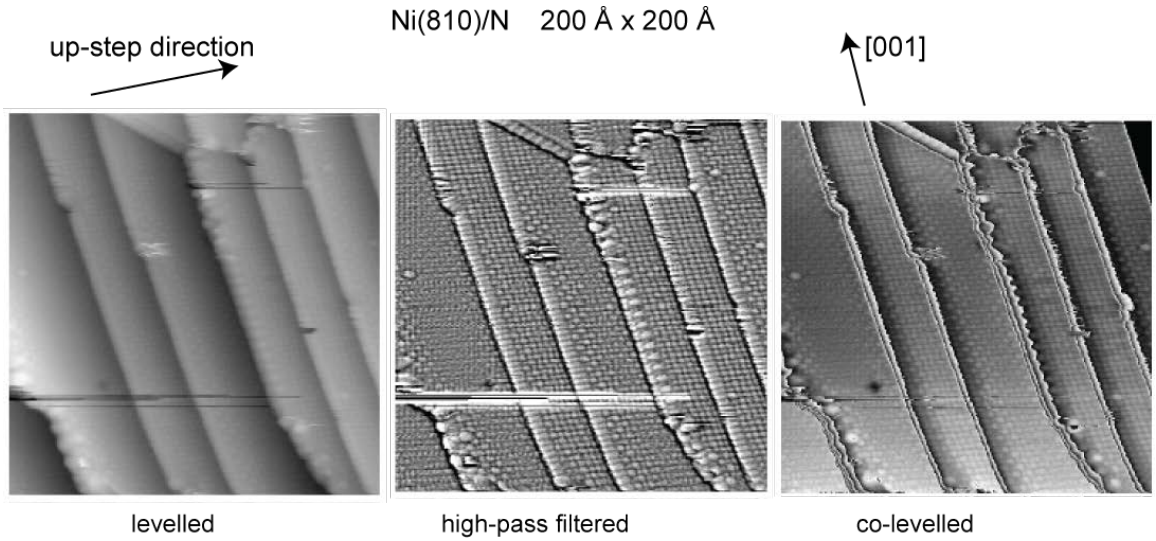

Fig. 3 STM image of a 200 Å x 200 Å area of a Ni(810)/N surface subjected to three different forms of image processing: levelling to the average surface plane, high-pass filtering, and 'co-levelling' to each (100) terrace, as described in the text. (-18 mV sample bias, 1.8 nA tunnelling current, 0° scan angle)

We have also made use of lattice averaging to gain a clearer picture of faint atomic scale detail in a few images that are specifically identified here as having been processed in this way. This simply involves adding each instance of the unit mesh within a selected region to form an averaged unit mesh in which the noise is reduced. This can then be tiled onto the original array of lattice points in order to visualise the long-range periodic structure.

3. Results

3.1 STM characterisation of step bunching and faceting

We first consider briefly the information gained from lower-resolution STM images of the nanometre-scale morphology of the surfaces. Fig. 4 shows some representative images, each corresponding to a 200 Å wide region, for all four surface/adsorbate combinations.

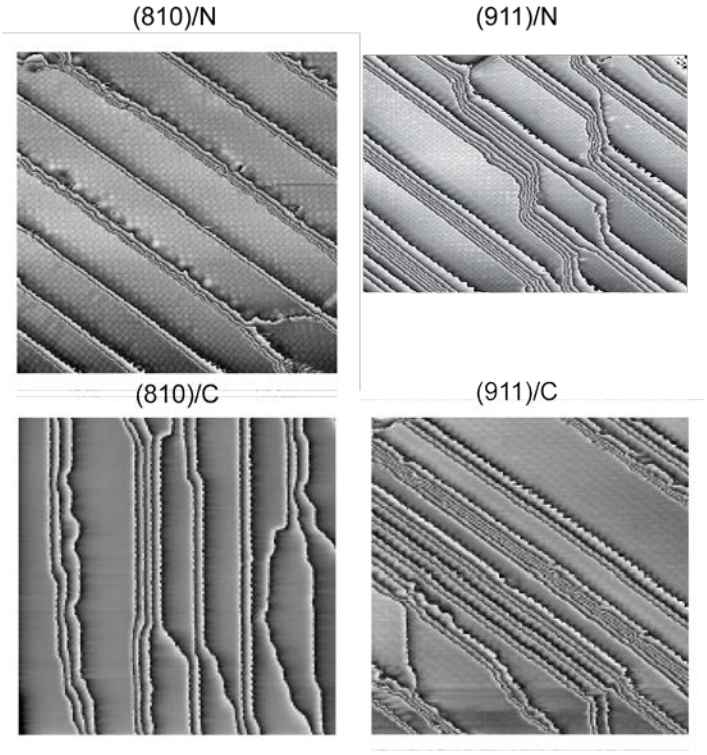

Fig. 4 STM images from four areas, each 200 Å wide, showing step bunching behaviour from: Ni(810)/N (-18 mV, 1.8 nA, -45°); Ni(911)/N (-99 mV, 1.7 nA, +45°); Ni(810)/C (-3.0 mV, 2.6 nA, +90°); Ni(911)/C (+14 mV, 1.5 nA, +45°) surfaces. Note the (810) images are recorded from two different samples mounted at different azimuthal orientations.

All surfaces show at least some tendency to step bunching, and most steps are relatively straight, aligned along either the [001] or [01$\bar{1}$] average step directions, but there are some more detailed variations in behaviour. In the case of Ni(911)/C surfaces, in particular, multiple step bunching dominates, with a strong tendency towards the formation of local (411) facets between the larger (100) facet regions. The ideal (411) surface actually comprises alternating narrow and wide (100) terraces of (311) and (511) character, but of course both these terraces are narrower than those of an ideal (911) surface (fig. 5). Ni(911) in the presence of N is also characterised by multiple step bunching, though in this case no facet orientations of intermediate orientation were observed, tight bunching to give an orientation approaching (111) being the norm.

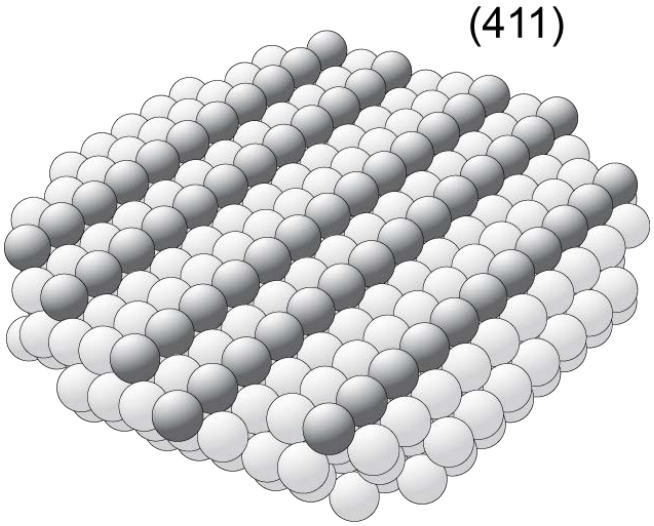

Fig. 5 Schematic diagram of an ideal Ni(411) surface. The atoms along the steps (the down-step edges of the terraces) are shaded darker for clarity.

On the Ni(810) surface, on the other hand, multiple steps separating terraces between 2 and 4 layers apart are more nearly the norm, although some cases of single and higher multiple step groups are seen. Interestingly, in cases where two groups of more than a pair of steps occur in close proximity, some isolated steps are seen to 'wander' between the two groups, losing their preferred [001] direction in these regions, switching between [001] and [01$\bar{1}$]. We also note that for Ni(810)/N, double-height steps are very regular (atomically straight) whereas higher (multiply-bunched) steps are markedly irregular (atomically rough) (Figs. 3 and 4).

Apart from the intrinsic, and potential practical, interest in this step-bunching and faceting behaviour, this does have some implications for the main focus of the present investigation, namely a study of the atomic-scale reconstruction of Ni(100) terraces on such surfaces. As different widths of terraces correspond to different constraints on the lateral strain which may occur as a result of adsorption, one would wish, ideally, to be able to image the structure as a function of position within an individual terrace (relative to the highly-constrained up-step and relatively unconstrained down-step edges of the terrace) and to perform this investigation on terraces of different widths. Step bunching in general leads to much wider terraces, but may also (as in the case of faceting of (911) to (411)) lead to much narrower terraces, and both of these may limit our study in some ways. In the case of the narrow terraces there is also a significant practical problem. Obtaining good atomic resolution images of metal surfaces is generally quite demanding, and for extended low index surfaces (the simplest situation) one requires a tip with a rather sharp protrusion on an atomic scale. Such a tip will also readily resolve the outermost step atoms of a vicinal surface, but to resolve detail on the terraces is more demanding. As one scans the tip across the terrace, from these highest atoms at the down-step edge towards the 'corner' presented by the up-step edge of the terrace, it is important that the tunnelling protrusion of the tip is long enough (relative to other protrusions on the 'end' of a tip that is blunt on this atomic scale) that it remains the only point of tunnelling. Clearly, the closer one approaches the up-step edge, the less likely this becomes. Achieving good atomic-scale resolution of narrow terraces (just a few atomic spacings wide) is therefore particularly difficult. However, even wide terraces do offer the possibility of establishing what the *local* effect of the less-constrained environment of the down-step edge may be on the structure, and because the overall morphology of the surface is undoubtedly not a true equilibrium state, there are local variations in step spacing that allow some terraces of intermediate width to be investigated.

3.2 The local structure of (100) terraces

3.2.1 Introduction

Before presenting the detailed results of the atomic-scale STM images of the different adsorption phases, it is appropriate to make a few general remarks regarding the nature of such images and their interpretation. Firstly, for an adsorption structure, which therefore comprises atoms of two (or more) different elements (in this case either C or N and Ni), one has the question of which atoms are imaged as protrusions in STM. In some cases even this question is too simple, because the STM protrusions (seen in constant-current mode imaging as used here) may even correspond to locations midway between surface atoms (e.g. [13]), but we will not consider this possibility further here. More significantly, it may be possible to obtain images of either atom by adjusting the tunnelling conditions or tip state. However, in the present case the tip state, and notably the presence or absence of specific adsorbate atoms at the tunnelling point, is somewhat unpredictable and ill-defined. Nevertheless, this possibility of imaging different atoms with accidentally 'functionalised' tips was demonstrated in early studies of O on Cu(110) [14] and N on Cu(111) [15], and indeed more recent studies of molecular adsorbates have exploited deliberate 'functionalisation' of a tip by adsorbing CO molecules onto it (e.g. [16]). In the case of C adsorbates, and C on Ni(100) in particular [5], it seems that C always appears in STM images as a dip rather than a protrusion, so atomic-scale protrusions are always believed to be associated with Ni atoms. In fact this same effect of the adsorbate appearing as a dip has also been predicted for N on Pt(111) [17]. However, in the case of N on Ni(100) an STM study [18] shows that at low (mV) bias voltages one sees protrusions in positions characteristic of the Ni atoms in a (2x2) clock reconstruction, whereas at high (0.5 V) bias a c(2x2) array of protrusions is seen in relative positions consistent with the locations of the N atoms. The majority of the images presented in the current paper were obtained at low bias voltages. In general, therefore, we expect our STM images of Ni(100) terraces on the vicinal surfaces to show Ni atoms, and not C or N, as protrusions. More specifically, any image in which the array of protrusions shows the full packing density of the outermost Ni layer, as opposed to that of the 0.5 ML overlayer of adsorbate atoms, can only reasonably be interpreted in this way.

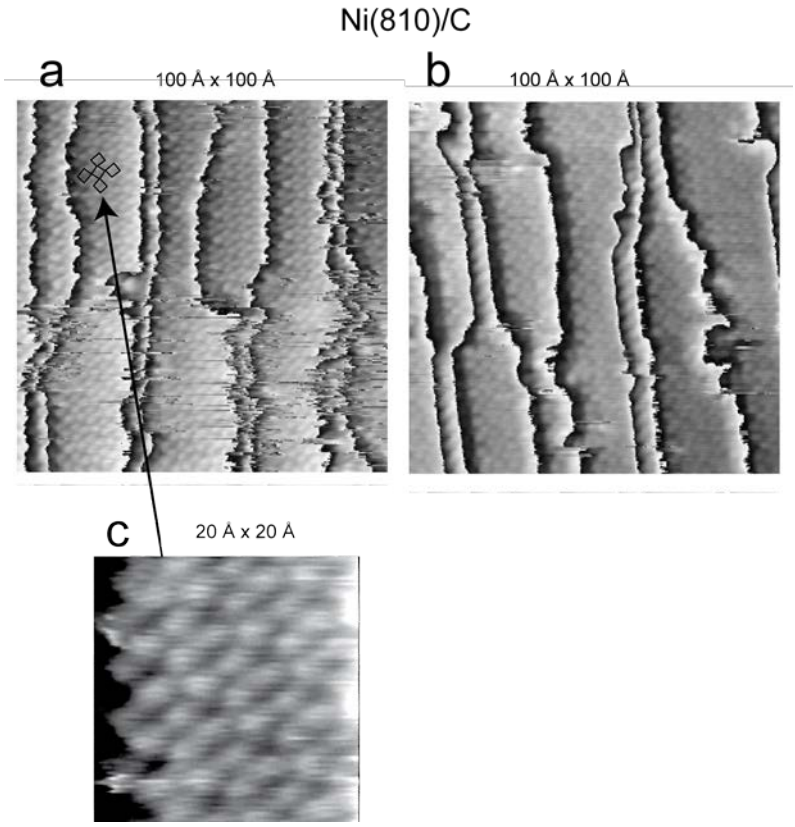

Fig. 6 Representative co-levelled STM images from 100 Å x 100 Å areas of the Ni(810)/C surface. The clock reconstruction is seen on all terraces, and a small section of this distortion is overlaid on the left-hand image. (a) +31 mV, 2.6 nA, 0°; (b) -2.4 mV, 2.6 nA, 0°. (c) shows an enlarged part of the image in (a) as indicated by the arrow

3.2.2 Ni(810)/C

Fig. 6 (a) shows a typical example of a high magnification image of an area of the Ni(810) surface after dosing with C. Within the terraces, the images show lateral distortions of the Ni atom positions that are the clear signature of the clock reconstruction (see superimposed lines on a small section of the left-hand image and also the enlarged part of this region in Fig. 6(c)), apparently identical to that seen on more extended Ni(100) surfaces. Notice that this is (mostly) true even for the narrowest terraces which appear to comprise only 5 or 6 [010] atomic rows. Establishing the nature of the reconstruction at the edges of the terraces, however, is difficult. We have already remarked on the potential difficulties of obtaining reliable atomic-scale imaging of the atoms on the up-step edge of a terrace due to the shape of the tip, but might anticipate that more reliable information may be obtained from the atoms on the upper edge of a step, corresponding to the down-step edge of a terrace. In Fig. 6, these regions lie just to

the right of the step lines, as the up-step direction of the surface is from left to right. To try to identify the behaviour at these terrace edges, we first note that, as seen in the model of the Ni(100)(2x2)-C pg clock reconstruction (fig. 1), the structure is composed of two inequivalent [001] (and [010]) atom rows. One of these includes the C atoms and has the Ni atoms displaced alternately to the left and to the right to produce a characteristic zig-zag appearance. The other row contains only Ni atoms, which are all perfectly aligned but which have inequivalent spacings that are alternately long and short to produce a kind of atom pairing. Inspection of the images of Fig. 6 shows that in most (though not all) of the step regions, the last bright row of protrusions to the right of the steps exhibits pairing that appears to correspond to this latter type of row. However, the mid-step line, where the sharp black-white transitions occur, is significantly displaced to the left of these bright rows. Based on the periodicity of the rows perpendicular to the steps, it seems that there should be one further row of Ni atoms at the down-step edge of the terrace that are not visible, presumably because of the Smoluchowski smoothing of the valence electron density at the step, such that the valence charge density drops at these terrace-edge atoms. In fact, at some terrace edges, there is some indication of weak protrusions in this region, but the details are unclear. This discussion implies that the true terrace-edge atom row corresponds to one in which, at least if it were in the mid-terrace region, there should be a row of C atoms. We may therefore suggest that there are most commonly C atoms in the reduced coordination sites at the step (although the C atoms, of course, are not actually seen in the images). Adsorbate occupation of these sites is exactly the situation found for the Cu(410)/O surface, although in this case the O atoms actually appear to prefer these step sites to the mid-terrace sites (e.g. [26] and references therein).

LEED patterns recorded from this surface showed the expected (2x2) diffracted beams and also indicated that the (½ 0) and (0 ½) beams were systematically absent at normal incidence, consistent with the pg space group symmetry of the clock reconstruction. However, careful inspection showed that very weak features could be seen at these locations in the diffraction pattern at certain energies; it is possible that this may be a consequence of a slightly off-normal incidence geometry, but it may simply reflect that

fact that the predicted extinction should only be strictly valid for an extended (nominally infinite) (100) surface.

3.2.3 Ni(810)/N

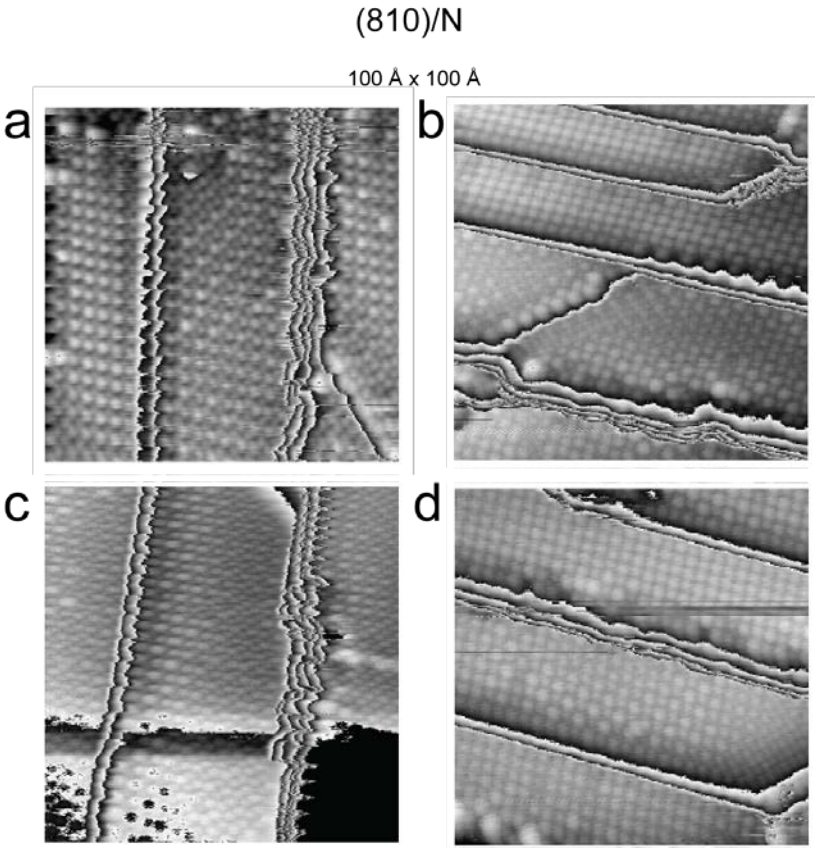

Fig. 7 Representative co-levelled STM images from the Ni(810)/N adsorption system from 100 Å x 100 Note the sample is rotated azimuthally by ~75°Å areas. between the left and right-hand pairs of images. (a) -58 mV, 2.4 nA, +90°; (b) -18 mV, 1.8 nA, -75°; (c) -1.0 V, 2.8 nA, +90°; (d) -18 mV, 1.8 nA, -75°

Fig. 7 shows a set of four representative higher magnification images from the Ni(810)/N surface. The appearance of the (100) terraces is clearly not simply of complete clock reconstruction, and indeed there appear to be several distinct types of behaviour. These differences cannot be attributed to tip effects, as they can be seen between adjacent terraces within the same image, and even between different regions of the same terrace. Certain regions within these images do show lateral distortions of the Ni atoms characteristic of the clock reconstruction; see, for example, the upper half of the central terrace in Fig. 7(a), shown enlarged in Fig. 8(b), but also the centre terrace of fig. 7(b) towards the right-hand side (approaching the up step). By contrast, in the left- and right-

hand terraces of Fig. 7(a) there is no systematic lateral distortion, and the density of the major protrusions is reduced by a factor of 2, corresponding to a c(2x2) periodicity. An enlarged image of the left-hand region is shown in Fig. 8(e).

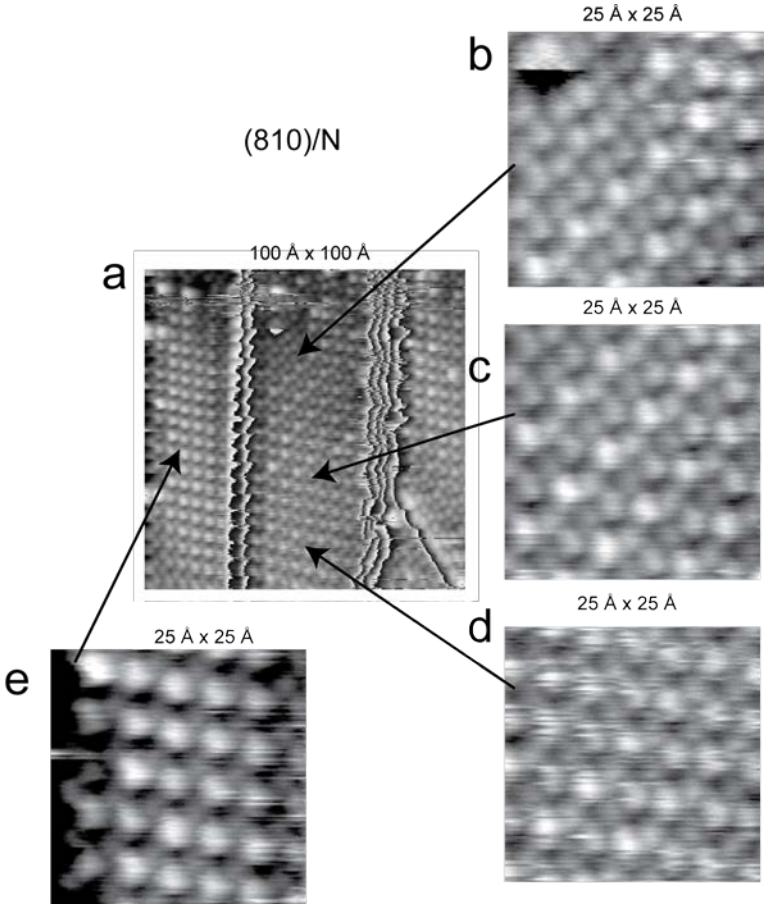

Fig. 8. (a) shows the same image as in Fig 7(a) while ((b) to (e) show enlarged images of four different regions of (a) as indicated by the arrows.

Careful inspection shows that weaker protrusions do appear at the centre of each group of four nearest neighbour strong protrusions, suggesting that there is a periodic variation in the height of the Ni atoms such as to produce a c(2x2) rumpling. A degree of vertical rumpling is also apparent within the clock-reconstructed regions in some cases. In the centre terrace in fig. 7(a), for example, shown enlarged in Fig. 8(c), there appears to be a (2x2) rumpling in the central part of this terrace that merges into a c(2x2) rumpled structure in the lower part of the terrace (enlarged in fig. 8(d)); this resembles the c(2x2) structure on the adjacent terraces, but retains the lateral distortions of the clock reconstruction (and so is strictly (2x2) in its periodicity).

The remaining two images on Fig. 7 in panels (c) and (d), (of marginally lower resolution) are from a separate set of measurements in which the crystal was mounted in the sample holder in a different azimuth such that the main step direction of the surface is rotated by approximately 75°. In these images, too, most areas of the terraces show a c(2x2) periodicity of the imaged protrusions, although both images also contain terraces in which lateral distortions characteristic of the "c(2x2)-rumpled" clock structure can be seen. A possible clue to the origin of this structural variation can be seen in the terrace just above the centre of the image of Fig. 7(c); at the point where the terrace widens, the rumpled c(2x2) structure without lateral distortions gives way to the rumpled c(2x2) structure with lateral distortions consistent with clock reconstruction. This example is complicated by the fact that the down-step height also changes in the centre of the image, introducing step irregularity. Nevertheless, our images do indicate a broad correlation between terrace width and the propensity for lateral distortions to be seen, suggesting that the clock reconstruction (albeit with some degree of vertical rumpling) switches on when the terraces reach a width of around 15 [001] rows, but is absent in narrower terraces.

Also shown in figs. 7(a), (c) and (d), however, are regions in which a single step switches between two [001] step bunches, adopting a $[01\bar{1}]$ direction at 45° to the other steps. The structure of the terraces in these regions appears significantly different. In terrace regions close to these $[01\bar{1}]$ steps there is clear evidence of a higher density of protrusions, consistent with the (1x1) density of the surface Ni atoms, and with some evidence of the pairing and zig-zagging of protrusions characteristic of the clock reconstruction. There are also a few particularly large protrusions close to the steps in these images, but it is difficult to draw conclusions from such isolated observations.

The presence of a c(2x2) phase would actually be consistent with the results of an earlier LEED study of Ni(100) vicinals in this [001] zone [11] that found there was no clear evidence of the (2x2) periodicity characteristic of the clock reconstruction for vicinals more than about 2° from (100). However, our own LEED experiments from this surface do show a clear (2x2) pattern, once again with extremely weak (½ 0) and (0 ½) beams. In fact these beams were found to have somewhat more intensity than those from Ni(810)/C

in at least one narrow energy range around 90 eV, but in this case too it is possible the origin of the effect is symmetry breaking by the small terrace domains. Of course, the fact that we see some regions of clock reconstruction in the STM images means that we would expect to see a (2x2) LEED pattern. The diffracted beams of a c(2x2) mesh are a subset of those of the (2x2)pg phase, so there would be no qualitative difference in the LEED patterns from pure (2x2) and mixed phase (2x2)/c(2x2) surfaces. Why the earlier LEED study showed none of the additional p(2x2) diffracted beams is unclear, but our own STM results clearly show some variability of the surface structure, so it is certainly possible that slightly different methods of preparation favour different relative amounts of the two phases.

What is far less clear, of course, is what the nature of the c(2x2) surface phase might be. The most direct interpretation of the STM images is that there is a periodic rumpling reconstruction of the outermost Ni layer. Just this type of rumpling has been proposed to be a characteristic of the Cu(100)c(2x2)-N surface [19, 20], although the interpretation of the associated STM images which provided one piece of evidence for this effect have proved controversial [21, 22, 23]. We will return to this question in the general discussion.

3.2.4 Ni(911)/C and Ni(911)/N

While the experiments on the Ni(810) with adsorbed C or N yielded images in which the clock reconstruction was clearly observed under certain conditions, albeit with evidence for coexistent c(2x2) regions, similar studies of the Ni(911) surface led to less clear-cut systematics, despite extensive investigation. In the case of STM studies of the Ni(911)/C system, we have already described the tendency to produce arrays of rather narrow (100) terraces characteristic of a (411) orientation. The local reconstruction behaviour of such narrow terraces, even if we could resolve it in STM, would not form a basis for understanding the influence of the step orientation on wider terraces such as those we have characterised on the (810) surface. We have therefore concentrated on those images of the (911) surface that reveal atomic-scale detail of the small number of intermediate

width terraces that survive. Fig. 9 shows two such examples. Fig. 9(a) and (b) show images of two 100 Å x 100 Å regions, while (c) and (e) show magnified images extracted from the largest terrace region in each image. These enlarged images are quite noisy, but (d) and (f) show lattice-averaged images extracted from these, leading to substantially reduced noise levels and much clearer images. The narrow terrace seen in fig. 9(a) clearly shows atomic protrusions with a density consistent with the (1x1) periodicity of the Ni substrate, but in the magnified and lattice averaged image it is clear that there is actually a (2x2) periodicity. The larger terrace in fig. 9(b) also shows a (2x2) periodicity, albeit of a quite different character.

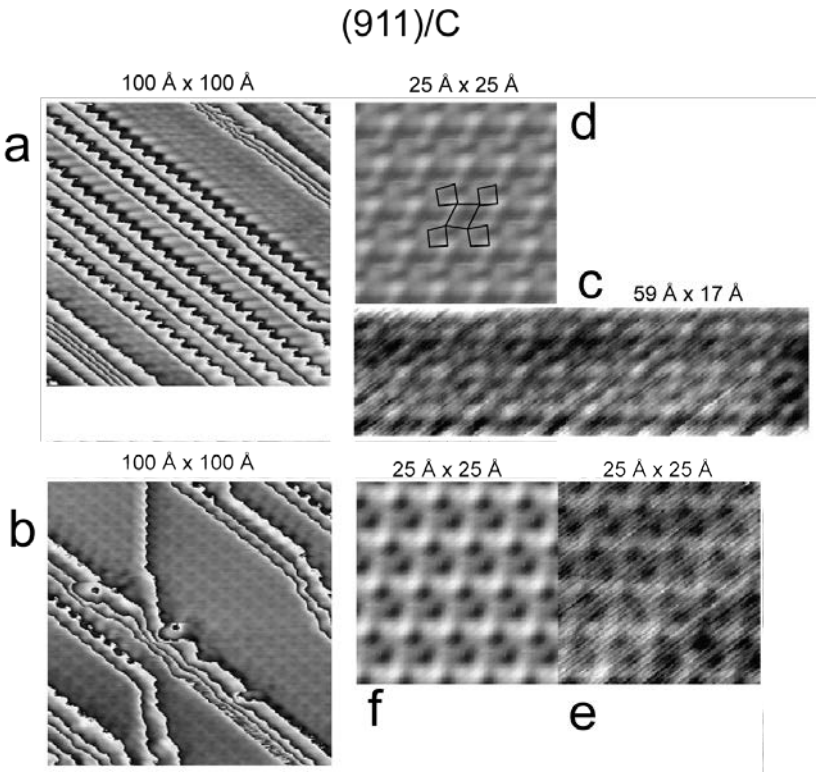

Fig. 9 (a) and (b) show co-levelled STM images of two 100 Å x 100 Å areas of the Ni(911)/C surface, while (c) and (e) show magnified (and rotated) images taken from the largest (100) terrace in each of these images. (d) and (f) are lattice-averaged images extracted from (c) and (e). Superimposed on (d) is a distorted motif similar to that of the clock reconstruction of fig. 1. (a) -3.4 mV, 1.5 nA, +45°; (b) +14 mV, 1.5 nA, +45°.

Comparison of the two lattice-averaged and magnified images (fig. 9 (d) and (f)) show some similarities, but also significant differences. Both show a (2x2) array of bright features, which appear as single atomic protrusions in Fig. 9(d), but which are heavily streaked along the sides of the (2x2) mesh in Fig. 9(f). The image of fig. 9(d) shows 4

atomic protrusions per unit mesh, albeit of different heights, consistent with the expected 4 Ni atoms in the (2x2) periodic structure. There are clear lateral distortions, with some zig-zag rows; if one tries to map the relative positions of the protrusions (superimposed on the image) one obtains a motif similar to that of the clock reconstruction, but very significantly distorted. Of course, the pronounced differences in apparent height of the protrusions are also uncharacteristic of a true clock reconstruction.

Apart from the (2x2) square grid of bright lines that characterises the appearance of the image of fig. 9(f), the other striking feature is the two dark depressions in each square. This would define a nominal c(2x2) mesh, but for the fact that they are clearly not truly periodic, showing a 'pairing' in one <001> direction and a zig-zag appearance in the orthogonal direction. As remarked earlier, C on Ni(100) images in STM as depressions, which in the clock reconstruction are arranged on a regular c(2x2) mesh, so it is tempting to associate these depressions in fig. 9(f) with C atoms in the same way, but if this is correct, the fact that they are not on a regular c(2x2) mesh clearly means that the image is not of a simple clock reconstruction.

Superficially, at least, the images of fig. 9 suggest that the (100) terraces of Ni(911)/C are most typically found to produce one of two rather different (2x2) reconstructions involving some kind of lateral reconstruction. We should note, however, that different tip conditions in STM can lead to images of the same surface structure that appear significantly different; it is certainly possible that the two types of images in fig. 9 are a consequence of this effect; specifically, both types of image show (2x2) periodicity, lateral distortion, and some kind of corrugation perpendicular to the surface. However, neither is consistent with a simple clock reconstruction.

LEED from this surface showed a streaky (2x2) pattern that did appear to show significant intensity in the (½ 0) and (0 ½) beams, although the strong streaking, presumably a reflection of the large variations in step spacing and terrace width, made it difficult to be sure that this effect was significant. The appearance of such ‘forbidden’

beams would provide further evidence that a (2x2) phase other than the clock reconstruction occurs.

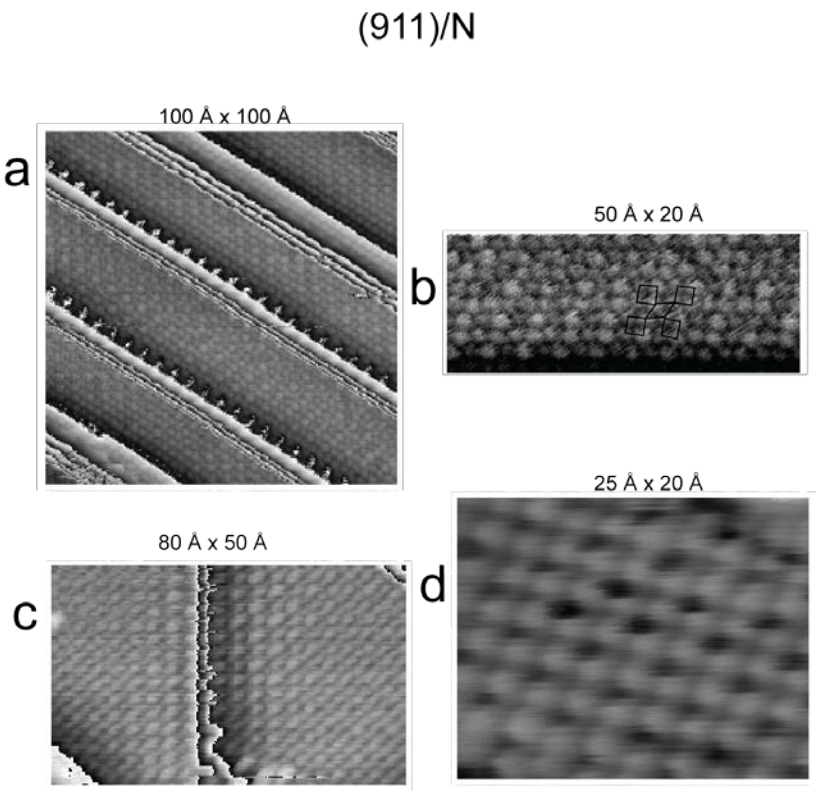

Fig. 10 STM images of the Ni(911)/N surface. (a) shows an area of 100 Å x 100 Å while (b) shows on an expanded scale a single terrace from this image. (c) and (d) show representative images from two other areas, (d) being a higher magnification image of part of a single (100) terrace. Superimposed on (b) is a distorted motif somewhat similar to that of the clock reconstruction of fig. 1. (a) +57 mV, 1.3 nA, +45°; (c) -1.5 mV, 5.0 nA, +45°; (d) -0.28 mV, 5.6 nA, +15°

Fig. 10 shows some representative STM images from the Ni(911)/N surface. Fig. 10(b) shows an expanded image of a single (100) terrace from fig. 10(a), but the other images are of different regions at various magnifications. Fig. 10(d) shows the simplest behaviour; bright protrusions define a (1x1) mesh while the dark depressions define a c(2x2) mesh. This image is entirely consistent with an unreconstructed c(2x2) N overlayer phase with the N atoms occupying the hollow sites if we assume, as argued earlier, that under the tunnelling conditions used in these experiments N atoms (like those of C) will image as depressions. The images of the terrace(s) in fig. 10(a) and (b) are somewhat less clear, showing an array of bright protrusions on a nominal (1x1) mesh consistent with the surface Ni atomic density, but no clear pattern of depressions is seen.

On the other hand, some lateral distortion is clearly visible in the images that, combined with a slight variation in the height of the protrusions, is seen to correspond to a (2x2) periodicity. Superimposed on this structure is a motif somewhat similar to that of the clock reconstruction, but comparison with that of the true clock reconstruction (comprising counter-rotated squares) shows that this distortion is clearly quite different – indeed, it also appears to differ significantly from that seen in fig. 9(d) from the same Ni(911) surface in the presence of chemisorbed atomic C.

Fig. 10(c) shows an image from a different area of the surface, but the azimuthal orientation of the crystal and scan angle are the same as in fig. 10(a), so the double-step running from top to bottom is not in the $[01\bar{1}]$ direction which characterises the (911) surface, but rather in a [001] direction (the direction of the principle steps on the (810) surface). As such the behaviour on the terrace bears a significant resemblance to fig. 7(b) from the (810)/N surface. Specifically, close to the double step and on *both* sides (i.e on both the up-step and down-step edges of the adjacent terraces) the dominant appearance of the image is of a c(2x2) array of protrusions, while a few atomic spacings away from the steps it appears that all the surface Ni atoms are imaged as protrusions in a laterally-distorted structure very similar to that seen in fig. 10(b).

4. Discussion

Our results show three general features. Firstly it is clear that both C and N adsorption on both the vicinal surfaces studied (with steps aligned in the two distinct principal directions, [001] and $[01\bar{1}]$) lead to step bunching. On the Ni(810) surface double, triple and quadruple steps are most common, whereas on Ni(911) multiple step bunches lead to faceting to (100) and, in the case of C adsorption, to (411). It was not possible to obtain any detailed atomic-scale imaging of the very narrow terraces on the (411) facets which might give some insight into the special stability of this step spacing, and with little understanding of the anisotropy of the surface free energy of adsorbate-covered surfaces, it is difficult to comment on these results further. An investigation of the equilibrium

shape of small carburised Ni crystals at 1200°C [24] did not show any (411) facets on the surface, but the conditions of this experiment were very different from our own.

The second clear result from the STM images is that on Ni(810), with both C and N adsorbates, a (2x2)pg clock reconstruction is seen on the (100) terraces, although the situation is less clear on the Ni(911) surface; on Ni(911) there is evidence for laterally-distorted structures with (2x2) periodicity, but the detailed arrangements appear to be distinctly different from the clock reconstruction. A third result, however, is that these images also provide evidence for at least one other c(2x2) type of adsorbate-induced reconstruction on some (100) terraces or parts of them. While this was one of the qualitative effects which we sought to establish, the apparent nature of the modified reconstruction in terms of atomic movements perpendicular, rather than parallel to the surface (partially unconstrained laterally) was not expected. Here we consider firstly the way in which a stepped surface might be expected to influence the clock reconstruction, and secondly what possible structural models which might account for some of the STM images which do not correspond to those expected for a clock reconstruction. Our discussion is based on the assumption that it is the role of adsorbate-induced surface stress (known to occur to for C and N adsorption on extended Ni(100) surfaces), and the possibility of stress relief at step edges, that may account for the different structures seen on the narrow (100) terraces of the stepped surfaces. Of course, the electronic structure at surface steps also differs from that of the extended (100) surface but the most significant such difference, the dipole moment at the steps, is unlikely to strongly influence the adsorption behaviour of atomic adsorbates in the way that may be expected for molecular adsorbates with their own significant dipole moments. Notice that the different local reconstructions that we observe are quite different from the apparent [4] distortions [5] seen at lower coverages of C on extended Ni(100) surfaces, so there is no reason to believe that their origin lies in a lower C or N coverage on the narrow (100) terraces of the stepped surface.

As may be seen in Fig. 1, a characteristic of the clock reconstruction is displacements of the surface layer Ni atoms in the [010] and [001] directions in the surface. These

movements do cause some pairs of Ni surface atoms to become closer together than in the bulk solid, but the overall impact of near-neighbour distance reduction is minimised by the concerted nature of the movements on an extended (100) surface. The structure is also characterised by a significant rumpling of the second Ni layer with different layer spacings for the Ni atoms covered, and not covered, by an adsorbed C or N atom [2]. These Ni atom movements all preserve the four-fold rotational symmetry of the substrate.

Consider, now, a narrow terrace of (100) on a vicinal surface. On the down-step edge of the terrace, lateral Ni atom movements perpendicular to the step direction are essentially unconstrained. On the other hand, at the up-step edge, the surface Ni atoms lie adjacent to Ni atoms that are in the second layer below the next terrace, and are therefore more heavily constrained in their lateral movement in this same direction perpendicular to the step, so it is not clear whether narrow terraces are more or less favourable situations for the development of a clock reconstruction. However, one can expect that multiple-height steps may allow an even greater degree of freedom at the down-step edge than single-height steps. The (810) and (911) faces differ in their step direction. On Ni(810) the steps run along [001], parallel to one of the displacement directions of the clock reconstruction, but perpendicular to the other; on Ni(911) the step direction is $[01\bar{1}]$ and both lateral displacements of the clock reconstruction are at 45° to the steps.

In the case of Ni(810)/C, the STM images show all terraces to be clock-reconstructed, with no obvious difference in the magnitude of the distortion across the terraces. As remarked earlier, it is difficult to ensure that the atomic-scale STM images of the terraces are entirely meaningful very close to the steps, and especially at the bottom of an up-step, but as far as one can tell the reconstruction occurs right to both edges of the terraces. Indeed, in the case of the down-step edge, the images seem to indicate that that the edge row is typically one in which the Ni lateral movements are perpendicular to the step, probably with the terrace edge containing C atoms (similar to the presence of O atoms at the terrace edges of the Cu(410)/O) surface). Insofar as movements perpendicular to the terrace edge are unconstrained at the down-step edge, this termination seems reasonable. One further feature we should note is the exact width of the (100) terraces. If a terrace has

an even number of [001] Ni atom rows – such as on an ideal (810) surface, where there are 8 [001] Ni atoms rows on the terrace – and if the down-step edge row has displacements perpendicular to the step, then the up-step edge row would have displacements parallel to the edge, a potentially favourable situation as the adjacent Ni row below the step is strongly constrained against lateral movements perpendicular to the step. The rather irregular or atomically-rough character of the steps in the Ni(810)/C images makes it difficult to identify clear systematics in the terrace widths, but in those regions in which pairs of steps occur the number of terrace rows does appear to be even (mainly 8 or 10).

We now turn to the Ni(810)/N data, for which we also find terraces which are clock reconstructed. In addition, however, we see terraces which show a different reconstruction of apparent c(2x2) periodicity and even some terraces on which both phases occur in different regions of the same terrace, the c(2x2) phase apparently being favoured on the down-step side of the terrace. There appears to be a broadly systematic correlation with terrace width, the c(2x2) being characteristic of narrower terraces, whereas the clock reconstruction occurs on wider ones. Although in principle wider terraces may be expected to be associated with higher (multiply-bunched) steps, this is not systematically the case in practice. It seems that N can only induce the clock reconstruction if the terrace is more than around 15 [001] Ni atom rows wide, whereas on narrower terraces, c(2x2) rumpling occurs preferentially. Of course, the most obvious interpretation of a c(2x2) image in this situation would be that the STM is showing the adsorbed N atoms as protrusions. However, apart from the fact that our tunnelling conditions are generally similar to those previously found to favour Ni atom imaging [18], the fact that there are regions showing both c(2x2) images and (2x2) clock-reconstruction images on the same terrace (e.g. fig. 6 (b)) shows rather conclusively that these different local images cannot be due to changes in tip condition or tunnelling parameters. Interestingly, the regions of the surface showing the clock reconstruction yield images in which the magnitude of the apparent lateral distortion is generally smaller than that seen on the Ni(810) terraces in the presence of carbon. By contrast, the previously-published STM study of the Ni(100)(2x2)-N pg surface [18] shows apparent

distortions similar to those of published images from Ni(100)(2x2)-C pg [5]. Of course, the actual magnitude of the apparent distortion in these STM images cannot easily be related to the actual geometrical structural parameters, so it is not clear whether the amplitude of the N-induced clock distortion on the (810) terraces really is smaller than on an extended (100) surface, or whether the observed differences are a function of the exact tip condition. What seems hard to escape, however, is that two different local surface reconstructions can occur on Ni(810)/N, and that these probably have very similar energies.

In the absence of any further information one is obliged to interpret the STM image of the c(2x2) literally in terms of a periodic height variation of the surface Ni atoms, the main protrusions being the uppermost atoms while the lower ones give rise to the weak protrusions at the centres of the square mesh defined by the main protrusions. Fig. 11(a) shows this basic model; for clarity the outermost Ni atoms closest to the substrate are shown as spheres of smaller radius than those rumpled outwards. As noted above, evidence for such a structure (which has (reduced) two-fold symmetry) has been reported for Cu(100)c(2x2)-N [19, 20]. Fig 11(b) shows schematically how such a structure might evolve from a clock reconstruction as one approaches the down-step edge of the terrace to produce an STM image like that of the central terrace in fig. 7(b). In this figure the [001] lateral distortions of the outermost Ni atoms near the terrace edge have been removed, while those along [010] have been attenuated and moved outwards. Strictly the remaining distortion means that the terrace edge locally has a (2x2) rather than c(2x2) periodicity; in fact the STM image does suggest slight [010] distortion may remain on this central terrace of fig. 7(b). The fact that the atomic rows close to this down-step edge of the terrace are constrained along the [001] step direction, and not perpendicular to the step (along [010]) does make this type of lateral relaxation plausible, but why the layer should rumple is less clear. In the case of the Cu(100)c(2x2)-N surface it has been suggested that such a rumpling might provide an alternative means of relieving adsorbate-induced surface stress [19, 20], but of course we know that Ni(100) normally does so by a clock reconstruction. On the other hand, it is also known that relaxations perpendicular to the surface are generally larger on both clean and adsorbate-covered

stepped metal surfaces (e.g. [25, 26]), especially close to the down-step edge, than on the equivalent extended terrace surface orientation, so a rumpling reconstruction might be favoured in such a situation.

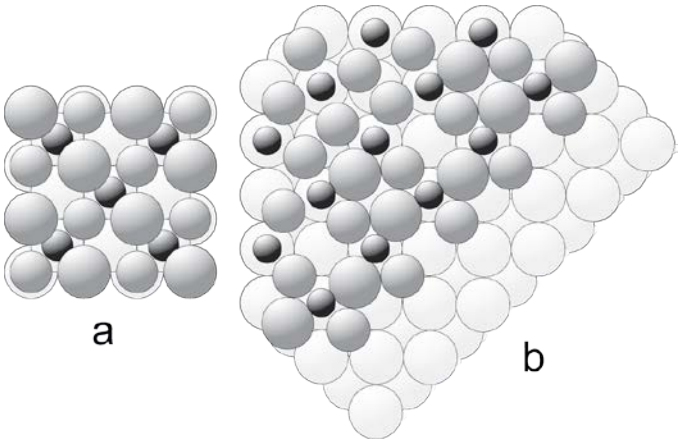

Fig. 11 (a) Schematic diagram of a model of a c(2x2) rumpled Ni(100)/N structure seen on some terraces of Ni(810). (b) schematic of a down-step terrace edge transforming from (2x2) clock to c(2x2) rumpled phase at the edge. N adsorbates are omitted from the lower terrace for clarity.

Perhaps the most notable feature of the results for the Ni(911) surface is that neither C nor N adsorption produced terraces that showed the clock reconstruction, although some regions of the surfaces do show a (2x2) periodicity (also seen in LEED) due to some kind of modulation of the basic feature of the images that comprise protrusions on a (1x1) mesh. Although some images (fig. 10(c)) show regions of c(2x2) protrusions similar to those seen on Ni(810)/N, they occurred where the local step direction was [001] and thus are really a further manifestation of the effect already described on Ni(810). Overall, the images of the (100) terraces of this surface are most readily understood in terms of a basic c(2x2)-N overlayer, with some evidence of lateral distortions, but certainly not those characteristic of a true clock reconstruction. The most obvious rationale for this effect is the constraint on lateral movements of the Ni atoms imposed by the up-step terrace edge, where outermost layer Ni atoms are adjacent to second layer Ni atoms below the next terrace. Notice that the lateral movements of the Ni atoms in the clock reconstruction are along [001] and [010]. For the nominal (810) surface, terminated by [001] steps, we have already argued that our images indicate that the edge [001] row of each terrace on the up-step side corresponds to movements along the step direction, and not perpendicular to it. On Ni(911), however, the steps lie along $[01\bar{1}]$, so in the clock reconstruction *all* atomic rows in this direction have a component of displacement

perpendicular to this step direction. If such motion is precluded for the up-step terrace edge, this may account for the lack of clock reconstruction.

5. Conclusions

Our investigation of the influence of N and C adsorption on Ni(810) and Ni(911) surfaces reveals not only some morphological effects associated with step bunching and faceting, but also atomic-scale STM images of individual (100) terraces. Both adsorbates are known to produce the (2x2)pg clock reconstruction on extended (100) surfaces, and both do induce this reconstruction on (100) terraces terminated by [001] steps, as provided by the (810) surface, although in the case of the N adsorbate a second coexistent c(2x2) phase is seen, most obviously reconciled with a Ni surface layer rumpling. On Ni(810)/C, on which terrace edge imaging proved to be easier, the terrace edge structure corresponds to [001] Ni zig-zag atom rows, indicating that the C atoms probably occupy the reduced coordination sites at the step (sites favoured by oxygen adsorbates on similar steps of Cu(100) vicinals). On Ni(911), however, the clock reconstruction was not seen on the (100) terraces and the STM images generally show protrusions on a (1x1) mesh with no obvious lateral distortions, although there is some evidence of a (2x2) periodicity which may be related to layer spacing variations. The absence of the clock reconstruction on these (100) terraces is suggested to be a consequence of the fact that the Ni atoms at the up-step edge of the terraces are prevented from moving perpendicular to the $[01\bar{1}]$ step direction by the adjacent second layer Ni atoms below the next terrace. By contrast, on (810) with an [001] step direction, this last Ni atom row need move only parallel to the step direction. Of course, in UHV surface studies of this kind the surface is never in a true equilibrium state, so some of the various structures we observe may be metastable rather than corresponding to true energy minima. On the other hand, one might expect the structure of narrow terraces to achieve local equilibrium more readily than that of extended (100) surfaces.

Acknowledgements

The authors acknowledge the support of the Engineering and Physical Sciences Research Council under grant number GR/L54172.

References

1 J.H. Onuferko, D.P. Woodruff, B.W. Holland Surf. Sci. 87 (1979) 357.

2 Y. Gauthier, R. Baudoing-Savois, K. Heinz, H. Landskron,, Surf. Sci. 251/252 (1991) 493.

3 M. Bader, C. Ocal, B. Hillert, J. Haase, A.M. Bradshaw, Phys. Rev. B 35 (1987) 5900.

4 R. Terborg, J.T. Hoeft, M. Polcik, R. Lindsay, O. Schaff, A.M. Bradshaw, R.L. Toomes, N.A. Booth, D.P. Woodruff, E. Rotenberg, J. Denlinger Surf. Sci. 446 (2000) 301.

5 C. Klink, L. Oelsen, F. Besenbacher, I. Stensgaard, E. Laegsgaard, N.D. Lang, Phys. Rev. Lett. 71 (1993) 4350 .

6 W. Daum, S. Lehwald, H. Ibach, Surf. Sci. 178 (1986) 528.

7 D.P. Woodruff in *The Chemical Physics of Solid Surfaces*, eds. D.A. King and D.P. Woodruff (Elsevier, Amsterdam, 1994) 7 465.

8 S. Stolbov, S. Hong, A. Kara, T.S. Rahman, Phys. Rev. B 72 (2005) 155423.

9 S. Hong, T.S. Rahman, J. Phys.:Condens. Matter 20 (2008) 224005.

10 D. Sander, U. Linke, H. Ibach, Surf. Sci. 272 (1992) 318.

11 J.C. Bouilliard, M.P. Sotto, Surf. Sci. 396 (1998) 107.

12 R.D. Kelley, D.W. Goodman, in: *The Chemical Physics of Solid Surfaces and Heterogeneous Catalysis*, Vol. 4, Eds. D.A. King and D.P. Woodruff (Elsevier, Amsterdam, 1982), p. 435.

13 S. Heinze, S. Blügel, R. Pascal, M. Bode, R. Weisendanger, Phys. Rev. B 58 (1998) 16432.

14 L. Ruan, F. Besenbacher, I. Stensgaard, E. Lægsgaard, Phys. Rev. Lett. 70 (1993) 4079.

15 S.M. Driver, D.P. Woodruff , Surf. Sci**.** 442 (1999) 1.

16 L. Gross, N. Moll, F. Mohn, A. Curioni, G. Meyer, F. Hanke, M. Persson, Phys. Rev. Lett. 107 (2011) 086101.

17 P. Sautet, Surf. Sci. 374 (1997) 406.

18 F. Leibsle, Surf. Sci. 297 (1993) 98.

19 J.T. Hoeft, M. Polcik, M. Kittel, R. Terborg, R.L. Toomes, J.H. Kang, D.P. Woodruff, Surf. Sci. 492 (2001) 1.

20 S.M. Driver, D.P. Woodruff, Surf. Sci. 492 (2001) 11.

21 T.E. Wofford, S.M. York, F.M. Leibsle, Surf. Sci. 522 (2003) 47.

22 S.M. Driver and D.P. Woodruff, Surf. Sci. 539 (2003) 182.

23 T.E. Wofford, S.M. York, F.M. Leibsle, Surf. Sci. 539 (2003) 186.

24 J.-S. Hong, W. Jo, K.-J. Ko, N.M. Hwang, D.-Y. Kim, Phil. Mag. 89 (2009) 2989.

25 Y. Tian, J. Quinn, K.-W. Lin, F. Jona, Phys. Rev. B 61 (2000) 4904.

26 E. Vlieg, S.M. Driver, P. Goedtkindt, P.J. Knight, W. Liu, J. Luedecke, K.A.R. Mitchell, V. Murashov, I.K. Robinson, S.A. de Vries, D.P. Woodruff, Surf. Sci 516 (2002) 16.